Published in final edited form as:
Minim Invasive Ther Allied Technol. 2010 August ; 19(4): 189–202. doi: 10.3109/13645706.2010.497000.

Toward adaptive stereotactic robotic brachytherapy for prostate cancer: Demonstration of an adaptive workflow incorporating inverse planning and an MR stealth robot

J. ADAM CUNHA[1], **I-CHOW HSU**[1], **JEAN POULIOT**[1], **MACK ROACH III**[1], **KATSUTO SHINOHARA**[2], **JOHN KURHANEWICZ**[3], **GALEN REED**[3], and **DAN STOIANOVICI**[4]

[1] Department of Radiation Oncology, University of California, San Francisco, CA, USA

[2] Department of Urology, University of California, San Francisco, CA, USA

[3] Department of Radiology, University of California, San Francisco, CA, USA

[4] Brady Urological Institute, Johns Hopkins University, Baltimore, MD, USA

Abstract

To translate any robot into a clinical environment, it is critical that the robot can seamlessly integrate with all the technology of a modern clinic. MRBot, an MR-stealth brachytherapy delivery device, was used in a closed-bore 3T MRI and a clinical brachytherapy cone beam CT suite. Targets included ceramic dummy seeds, MR-Spectroscopy-sensitive metabolite, and a prostate phantom. Acquired DICOM images were exported to planning software to register the robot coordinates in the imager's frame, contour and verify target locations, create dose plans, and export needle and seed positions to the robot. The coordination of each system element (imaging device, brachytherapy planning system, robot control, robot) was validated with a seed delivery accuracy of within 2 mm in both a phantom and soft tissue. An adaptive workflow was demonstrated by acquiring images after needle insertion and prior to seed deposition. This allows for adjustment if the needle is in the wrong position. Inverse planning (IPSA) was used to generate a seed placement plan and coordinates for ten needles and 29 seeds were transferred to the robot. After every two needles placed, an image was acquired. The placed seeds were identified and validated prior to placing the seeds in the next two needles. The ability to robotically deliver seeds to locations determined by IPSA and the ability of the system to incorporate novel needle patterns were demonstrated. Shown here is the ability to overcome this critical step. An adaptive brachytherapy workflow is demonstrated which integrates a clinical anatomy-based seed location optimization engine and a robotic brachytherapy device. Demonstration of this workflow is a key element of a successful translation to the clinic of the MRI stealth robotic delivery system, MRBot.

Keywords

Robotic brachytherapy; prostate cancer; adaptive workflow; seed location

Correspondence: J. Adam Cunha, Department of Radiation Oncology, University of California (USCF), San Francisco, CA, USA. CunhaA@radonc.uscf.edu.

Declaration of interest: The authors report no conflicts of interest. The authors alone are responsible for the content and writing of the paper.

Introduction

Over the past ten years approximately 400,000 men have been treated for localized adenocarcinoma of the prostate with permanent radioactive seed implantation as primary treatment. A series of steady and incremental improvements over the last twenty years has positioned prostate permanent-seed implants (PPI) among the most popular and efficient modalities to treat prostate cancer, offering one of the highest rates of local disease control (1–4). The success of brachytherapy1 is partly due to the constant technological progress in imaging modalities, dose planning, delivery techniques, and of skilled brachytherapy teams, allowing consistent seed insertion at pre-defined precise locations within the prostate. Brachytherapy has been in reported clinical practice for almost 100 years (5). Since the start of the modern era of brachytherapy which was marked by the use of pre-planned ultrasound-guided transperineal seed delivery as proposed and developed by Holm, in which images are acquired and seed locations determined by hand days before the implant procedure in the operating room (6), techniques have evolved toward adaptive quasi-real-time planning and seed delivery in the operating room (7).

However, based on long-term follow-up by experienced practitioners, approximately 30% of treatments fail biochemically (8). Patients treated by physicians who perform the procedure more often are less likely to experience recurrence or death from prostate cancer (9). Since the majority of procedures are performed by less experienced practitioners, upwards of 100,000 men might still experience a rise in the biomarkers indicating recurrence after a PPI procedure. Physicians have stated explicitly that attention to detail as well as an appreciation of the causative factors for the morbidity will help reduce treatment-related side effects (10). Biochemical control, for example, is directly related to the biologically effective dose actually delivered to the prostate (11). Thus, uncertainties are critical: Deviations from the ideal plan, organ motion, and the need to adjust and re-insert multiple needles (several times before reaching the proper position) all contribute to prostate edema and trauma to the surrounding tissues. Edema and trauma can cause side effects and/or jeopardize the prostate dose coverage and the implant effectiveness.

While a number of robotic hardware devices have been and will continue to be emerging from research labs in recent years (some of these are discussed below), a critical component of translating these devices into the clinic is establishing a clinically viable information workflow which integrates modern treatment planning software. A robotic approach for brachytherapy would have the potential to offer every man the opportunity to have a near-perfect seed implant by integrating the precision of the robot, anatomy-based dose optimization, and quasi-continuous imaging. However, while robots are very good at getting where they need to go, they lack the ability to know on their own where to go. The work presented here demonstrates the integration of a robotic brachytherapy system into a clinical workflow which can provide a robot with the where-to-go information.

In order to know where to go, physicians have employed a number of techniques. In the early days of brachytherapy, palpation and intuition were the main methods for determining where to place the radioactive seeds. This method is still used for some procedures, e.g. lining the surface of the cavity created when surgically removing a brain tumor (12). Modern brachytherapy uses a technique developed in the 1980s which employs transrectal ultrasound imaging to visualize the placement of radioactive seeds via the perineum (6). X-ray imaging was employed to evaluate the dosimetry, however only the bony anatomy was

[1]This term is derived from the Greek word “brachios” meaning short: brachytherapy consists of placing radioactive sources – about the size of a grain of rice – close to or inside a tumor or diseased organ. This contrasts with external beam radiation therapy in which radiation often must pass through healthy organs and tissue to reach the tumor.

visible on the 2D images (in contrast to the 3D reconstruction of soft tissue available with modern imagers). Therefore, an emphasis was placed on a uniform dose pattern. This *forward planning* technique emphasized minimal areas of high (hotspots) and/or low (coldspots) concentration of dose. With the improvement of imaging technology such that soft tissue was visible and organ delineation became possible, came anatomy-based dose planning. This method – now known as *inverse planning* in contrast to forward planning – is a technique in which all nearby organs are identified, digitized in a computer planning system, and expressly considered in the planning of the delivery of the prescribed dose.

Modern robot hardware now offers the ability to precisely insert a needle along any desired straight path in 3D space to reach a desired point consistent with prior imaging. This property – always knowing its exact position in space – is the defining characteristic of a *stereotactic* robot. Robotic needle insertion devices for performing biopsies are already being introduced in the clinic (13) and servo-type robotic surgical assistants like the da Vinci Surgical System, a device for laparoscopic surgery, have been installed in over 1000 locations worldwide (14). These kinds of servo devices have the potential to provide greater precision and accuracy compared to non-servo, unassisted surgery, and in many cases can be used with real-time and quasi-real-time imaging. Numerous other robotic hardware systems are being developed commercially and in academia for specialized medical procedures (15,16). Several groups have recently developed robots capable of operating in open (17,18) and closed (19–24) MR scanners, which is particularly difficult due to the limitations placed on robot materials by the magnetic field required for MR imaging.

To translate any robotic device from the workbench to clinic, it must be integrated with the treatment planning software used by modern brachytherapy clinics. The clinical workflow for prostate brachytherapy already consists of various hardware devices communicating with each other and the operators:

- Acquiring an image set of the patient anatomy,
- preparing a dose plan by determining the best location for the radioactive sources, and
- delivering the seeds via needles through the perineum into the prostate.

To bring a robotic device into a modern brachytherapy clinic, it is necessary to show that it can be integrated into this image/plan/deliver workflow. It would also be beneficial to show that a robotic device can expand the image/plan/deliver workflow into a fully adaptive procedure: Image/plan/begin-delivery/image/plan/finish-delivery (Figure 1).

The work presented in this paper demonstrates that this is achievable in a standard brachytherapy clinic using the same image-acquisition hardware and dose planning software as is used to treat patients on a daily basis. The use of the robot in two clinical environments is reported: An MRI unit and a brachytherapy suite equipped with a cone beam computed tomography system (CBCT). Both MRI and CBCT environments were used to demonstrate the links between various coordinate systems to enable this workflow: Image acquisition → Planning → Robot control → Robotic seed delivery. These experiments include the use of MR spectroscopic imaging (MRSI), CBCT, inverse planning (IP), and adaptive planning. The MRI was also used to demonstrate that functional imaging can guide the delivery of seeds (or biopsy), while the CBCT environment was used to demonstrate the adaptive planning and delivery process. The work detailed here demonstrates the ability to incorporate a robot into the information flow used in a modern brachytherapy clinic by integrating the robot's seed-delivery workflow with a clinically-used, image- and anatomy-based seed location optimization engine workflow in a manner that also allows for adaptive seed placement optimization.

Material and methods

Hardware and software

The experiments presented here integrate the adaptive planning and delivery process using a robotic brachytherapy seed delivery device into MR and CBCT environments. The robotic device was operated in a closed-bore 3T MRI system and a clinical brachytherapy suite equipped with a CBCT unit. Targets included inert ceramic dummy seeds, MR-spectroscopy-sensitive metabolite, and a prostate phantom. Acquired DICOM images were exported to a Windows XP PC running the treatment planning system (TPS), OncentraBrachy (Nucletron, Veenendaal, The Netherlands). The TPS was used to register the robot coordinates in the frame of the imager, contour imaged objects, verify target locations, create dose plans – including needle and seed positions, and export target coordinates (needle and seed positions) to the robot.

Robotic system

The MRBot system consists of the robot and its controller unit (Figure 2) (19). The controller unit includes a computer, motion control elements, a series of electro-pneumatic and electro-optical interfaces, and a brachytherapy seed magazine and delivery system. The robot fits into a standard closed-bore MR imager and is designed to interact with the patient inside the imager. The controller sits outside the MR imaging room and is connected to the robot by plastic hoses which carry air and fiber optic wires. To achieve full MR imaging compatibility, the entire robot is built of nonmagnetic and dielectric materials. The only metallic part of the robot is the MR imaging-compatible titanium needle. Standard hospital-room vacuum and air were used to operate the robot. The robot is built to operate on up to 120 p.s.i. Our hospital system operates on 60 p.s.i. At this pressure the actuator action of the pneumatic motor is about 50% slower than at 120 p.s.i., but the specs of the robot are otherwise unaltered.

A pneumatic actuator was specifically developed for this application. Unlike other types of pneumatic motors, this actuator uses a stepper motor's principle of operation and thereby achieves high precision in a safe and easily controllable manner (25). The linear size of one step is 0.055 mm. Pressure waves are used to set the motors in motion. These waves are created by a pneumatic distributor remotely located in the controller unit and are transmitted to the robot through the plastic hoses. The actuation is encoded by using fiber optics; the motors use pressurized air and light but no electricity.

To meet standard safety requirements for the use in medical applications, the robot's motors are designed for fail-safe operation. Any form of malfunction leads to a lock and cannot result in uncontrolled motion beyond the size of one step (0.055 mm).

The motors provide the robot with five degrees of freedom to place and orient an end effector (the tip of the robot in the foreground of Figure 2a as desired. The present end effector has one additional controlled degree of freedom to set the depth of the needle insertion, and three end-of-strike degrees of freedom to manipulate a titanium needle (18 gauge, 15 cm long) and to deploy brachytherapy seeds automatically (19).

In addition, this study takes advantage of the fact that the materials of the robot are fully compatible with a CT environment. The design uses only low-Z materials, and therefore produces minimal scatter from the robot itself during image acquisition (Figure 3).

For each set of seeds along one optimized needle2 path, the robot head is positioned at the entry point for that optimized needle. The robot needle is inserted to the desired depth and a seed is dropped, the robot needle is then partially retracted to reach the next seed position

and a seed is dropped. This is repeated for all seeds in the given optimized needle. Then the robot head moves to the entry point of the next optimized needle and the insertion process is repeated.

Imaging environments

MR imaging technique—All imaging studies were performed on a 3.0-Tesla whole body MR scanner (Signa; GE Medical Systems, Waukesha, WI, USA). Phantom/specimens were positioned inside of a Signa HD knee coil (GE Medical Systems, Waukesha, WI, USA) used for MR signal reception with the body coil being used for signal excitation3. MRI sequences acquired included a 3-plane fast single shot spin echo localizer (scout) with the following parameters TR/TE = 1300/85 ms, echo train length = 16, slice thickness = 5 mm, interslice gap = 3 mm, field of view = 35 cm, matrix 256 × 192. To check the positioning of the sample and prescribe the thin-section high spatial resolution axial spoiled gradient echo (SPGR) T1-weighted images the following were used: TR/TE = 16.5/3.3 ms, flip angle 12°, field of view = 35 cm, slice thickness = 1–2 mm, interslice gap = 0 mm, matrix 256 × 192. The high spatial resolution T1 weighted images were used to register the position of the robot in the coordinate frame of the 3T MR scanner using MRI visible markers installed on the nose of the robot and for targeting regions of interest for robotic needle placement.

For 3D Magnetic Resonance Spectroscopic Imaging (MRSI) needle targeting studies, a solution of 40 mM choline (Sigma-Aldrich, St. Louis, MO, USA) was injected into a 5 mm diameter cavity within the gel phantom. Elevated choline has been shown to be one of the most specific metabolic markers of prostate cancer (27). Localized 1H spectroscopic data were acquired using a spin-echo point-resolved spectroscopy sequence with 3D phase encoding. Data sets were acquired as 16 × 8 × 8 phase-encoded spectral arrays, with a TR/TE of 1,000/130 and a 17-minute acquisition time (26). In post-processing, the spatial resolution was interpolated from eight to 16 points in both the anteroposterior and cranio-caudal directions yielding a nominal voxel size of 0.09 cm^3. The choline peak area was numerically integrated and the resulting choline peak area images were zero filled to the resolution of the high spatial resolution T1 weighted images. Colored choline peak area contours were overlaid on the corresponding T1 weighted images and used for needle targeting. Since the 3D 1H MRSI data was acquired within the same exam using the same RF coils as the T1 weighted images, the metabolic and MRI data are already aligned.

Conebeam CT—A Simulix-Evolution™ CBCT simulator with an amorphous silicon flat panel detector with the Oncentra Simulation user interface (Nucletron, Veenendaal, The Netherlands) was used for the CT-based experiments. The following acquisition parameters were used: Full beam 100 kV x-rays at 16.0 mA with a imaging matrix of 512 × 512 pixels; slice thickness of 2 mm and using the built-in SmartScatter photon scattering correction.

Planning software

This TPS features two important characteristics necessary for quasi-real-time adaptive brachytherapy using a robot. First, it provides efficient DICOM image loading and manipulating functions. Second, all dose planning and delivery steps, including organ

[2]To be clear, the term *needle* is used in two different manners. (1) The optimization engine generates a dosimetry plan that consists of seed positions. These seed positions are relegated to sets which fall along a straight line. These sets are colloquially called needles because each set was inserted using one needle. (2) The robot itself has one needle that is used for the insertion of all the seeds. Where confusion may arise, *optimized needle* is used to refer to case 1 and *robot needle* to refer to case 2.

[3]The knee coil was used for phantom studies to provide good signal-to-noise imaging data for the relatively small phantom employed in these studies. For patient studies, excellent signal-to-noise can be achieved over the prostate and pelvis using the body coil for excitation and a combination of endorectal and pelvic phased array coils for signal reception. This coil combination produces sufficient signal-to-noise for the acquisition of spectroscopic and other functional imaging data from the prostate, and can be used with MRBot.

segmentation, catheter reconstruction, dose optimization, etc., are performed in the reference coordinate system of the DICOM images. All coordinate information for target locations were obtained through the clinical TPS software.

The TPS interfaces natively with the IPSA™ (28–31) inverse planning algorithm, which can be used for both high-dose-rate (HDR) brachytherapy and PPI. Although many of the characteristics of the robot are such that it can be used both for PPI and HDR brachytherapy, the experiments reported in this paper were performed for PPI. The TPS was used to perform the initial steps: Image loading, organ segmentation, and needle patterns. Organ contours and possible needle locations were then transferred to a research version of IPSA (similar to the version (28) available in the TPS, Spot-PRO, a PPI clinically available dose optimization and planning system)4. Dose constraints and organ contours were used by IPSA and optimal seed locations were determined. The resulting seed coordinates were then entered manually into the robot control system.

Results

Robot registration

To align the robot with the patient and the target anatomy, it is necessary to register the position of the robot in the coordinate frame of the imaging system. This procedure is the same for both the MR and CBCT systems. A special registration marker was installed on the nose of the robot. This marker is a continuous shape composed of an ellipse and a line segment (Figure 3d) and allows for the determination of the location and orientation of the robot's six degrees of freedom. Once the robot was fixed within the imager, an initial scout image was obtained to determine the gross positioning of the robot. The position of the markers was then registered using the scout image.

After the acquired volume was exported in DICOM format to the PC controller unit of the robot, the intersections of the markers with the planes of the MR sections were automatically identified and the registration transformation from the robot to the image was constructed using an automatic registration algorithm. This registration algorithm was previously developed and tested; it works with an intrinsic registration accuracy > 1 mm (32).

The registration of the robot reference frame to the reference frame of the imager is done only once throughout the procedure. This registration is valid until the robot is disassembled from the imaging couch or otherwise moved.

Single target in a homogeneous gel phantom—To verify the robot registration, an imagable target was created by hand placing a ceramic seed inside a gel phantom via a standard clinical PPI insertion needle. This phantom was then placed inside a Signa HD knee coil, and both were secured on the MRI bench. The robot was moved into position alongside the phantom and secured. The bench was then positioned inside the bore of the MR device. A scout image of the setup was taken to verify that the registration markers of the robot and the entire phantom were in the field of view of the imager. After the registration, a full-quality image was taken and exported in DICOM format to the planning system.

[4]The TPS environment used is designed for high dose rate (HDR) brachytherapy. Because the boundaries of the abilities of the treatment planning systems are being pushed, the older PPI treatment system made by Nucletron does not support the alternative needle patterns that are employed using this robotic device. However, the functionality of the TPS software necessary for the PPI planning done in these experiments is a subset of those necessary for HDR planning. The image processing, contouring, and optimization functionalities all exist on either system.

In this case, the ceramic target seed was digitized and its coordinates identified. The coordinates of the ceramic seed were then chosen as the target coordinates for the placement of a seed by the robotic device. The planning system coordinates were then translated into the robot's coordinate system and transferred to the robot's control system by hand. With the coordinates of the target now synchronized with the coordinates of the gel and the ceramic seed, the robot was instructed to place the seed. The result can be seen in Figure 4b and c.

Single target in bovine muscle—To verify accurate seed placement in a non-homogeneous environment, the same experiment was performed using bovine muscle. An imagable target seed was placed by hand in the sample. This was then placed inside the knee coil and attached – along with the robot – to the bench. The robot location was registered and an image set was acquired. The target seed was visible and is indicated by the arrow in Figure 5a. The needle that was used to place this seed by hand entered from the right-hand side of the image. The target seed was digitized and its coordinates were transferred to the robot. The robot's needle was inserted to the target location. A new image set was acquired to verify the location of the needle. The tip of the needle can be seen at the target location in Figure 5b. Note the larger MR signal (black circle) of the titanium needle tip. The seed was then deposited and the needle retracted. A final image set was acquired. The deposited seed can be seen in Figure 5c. Note the cylindrical extension of the black region at the robot-placed location. This is a result of the robot's seed driver mechanism: When inserting the seed a small pocket of air can be pushed ahead of the seed. This is not unique to this robot's delivery mechanism; it also occurs during the standard clinical hand placement of seeds. This pocket of air filled the cut in the tissue made by the needle which placed the target seed (the target seed's needle was inserted from the upper right portion of the tissue sample).

MRSI-based target—Since MRSI-based planning is also of interest, a registration and targeting test was run using MRSI information. MRS-imagable metabolite was placed in a gel phantom which was subsequently scanned. The MR images were then analyzed using the technique discussed above. The target coordinates were identified using the MRS information and transferred to the robot. A dummy seed was placed by the robot at the MRS-defined target location (Figure 5d and e). The seed was placed within 3 mm of the target.

Upon completion of the registration studies portion of these experiments, the use of a human prostate phantom (CIRS Model 053-MM (33)) was initiated. The goal here was to evaluate the range of motion of the robot and determine its ability to deposit seeds in a human-sized prostate. An MR image set of the prostate phantom was acquired and transferred to the TPS where the prostate and urethra were contoured. An apex location was chosen (in this case it was located outside of the phantom) and a cone-based implant using three needles and 11 seeds was generated. The range of motion of the robot allowed the necessary access to the prostate gland.

CT-based studies

In this phase of the experiment, the feasibility of clinically deploying image-guided robotic, inverse-planned (IGRIP) brachytherapy was explored using the MR stealth robot and the ability to link the CBCT images, the planning system, the robot control, and the robot in an information workflow was demonstrated. Because the CBCT system has an open architecture (Figure 6), visual and mechanical access to the robot and target can be obtained without moving the system. This is not true for the closed bore of the MR system.

To demonstrate adaptive dose planning, a CBCT of a prostate phantom was acquired and contoured. The setup is shown in Figure 6. The specific elements of the workflow used for these studies are:

- Obtain an image the target,
- transfer the images to the treatment planning system,
- generate the treatment plan (either by hand or using IPSA),
- send seed and needle position information to the robot control device,
- execute the robot control commands for positioning the end effector in the correct orientation for insertion of the needle,
- verify the end effector placement and trajectory by eye to confirm proper gross orientation and position,
- execute the commands to insert the needle and drop the seeds.

Up until this point all the steps completed are the essence of IGRIP brachytherapy and are performed whether or not an adaptive procedure is desired. To implement the adaptive portion of the workflow, the following elements were included:

- re-image the target after a given number of needles have been inserted and seeds placed,
- re-evaluate the treatment plan to determine actual seed locations,
- evaluate dosimetry and determine if re-optimization is necessary,
- repeat the above steps for every intra-operative image set obtained.

For this study, IPSA was used to generate a seed plan based on a needle pattern that used four entry points. Each entry point was used as the apex of a cone within which two or three needles were placed. Coordinates for ten needles and 29 seeds were transferred to the robot. After every two needles placed, an image of the phantom was acquired. The already-placed seeds were identified and validated prior to placing the seeds of the next two needles. Figures 7a–g show successive sagittal images of the phantom after every two needles. The first two images show the robot head with the needle extended.

Discussion

As mentioned in the introduction, a number of novel robotic brachytherapy devices will be leaving the lab and heading toward the clinic. Each system has its strengths and weaknesses. Of particular interest for all these systems is the technology to (1) introduce needles into the body causing minimal distortion of the organs and their relative position and orientation and/or (2) compensate for these changes. For example, Moerland et al. have discussed a robot (23) that minimizes distortions by utilizing a tapping method. The robot discussed here uses a very fast insertion stroke to take advantage of the rest inertia of the organs to minimize distortions on insert. Item 1 touches on an area of research that hopefully will produce results beneficial to the field as a whole – namely modeling of the needle-tissue interaction – and there have been some promising results including the results of (34) and that for curved needles (35). Of interest in this paper however is addressing item 2 and compensating for these inevitable changes via an adaptive planning workflow.

To make this transition successful and to fully tap the potential these robotic devices have to offer, a clinical workflow must be developed that can incorporate seamlessly these devices. This work here accomplished precisely this. The workflow demonstrated here incorporates

the robotic hardware, imaging devices, and planning systems into a procedure that takes full advantage of the software planning abilities of a modern brachytherapy clinic. Designing and building a robotic brachytherapy device is a significant accomplishment. But in order to be used efficiently and effectively in the clinic, the robotic device must be able to communicate with other hardware, imaging and planning software, and the human operators of these devices. This workflow demonstrates a method for achieving this synergy: A synergy that will allow for further improvement in brachytherapy care.

Reducing uncertainties is critical to further advancement of brachytherapy. In addition, the range of therapeutic outcomes reported in the literature is wide – ranging from the upper ninetieth percentile for recurrence free survival to as high as 30% biochemical failure. This dichotomy may be a result of a correlation between physician skill and therapeutic outcome for prostate permanent-seed implants. Placing seeds accurately and precisely is a skill which takes years of practice to hone, but is also the key factor in mitigating the radiation-induced side effects that are common after brachytherapy treatment.

The most common prostate brachytherapy practice incorporates the use of a regularly-spaced template for the positioning of needles and seeds. One of the benefits of incorporating a robotic device is the ability to remove this template from the clinical workflow. Without the restriction of a fixed template more degrees of freedom are available for the insertion of the needles or catheters (36–39). It has been shown (40) that this may aid in reducing the deleterious side effects that can be caused by trauma to the critical structures near the penile bulb like the cavernous arteries along the side of the penile bulb (41), by increasing the ability to avoid these structures.

A stereotactic robotic device will also mitigate this needle puncture trauma. This robot and the workflow presented here will have the largest impact in those clinics where the physician is new to the field or lacks the decades of experience necessary to master the art of brachytherapy seed placement. During a PPI procedure, it is not uncommon for the physician to have to insert each needle multiple times in an effort to ensure it is in precisely the correct position for the deposition of the seeds. Clearly in the hands of well established physicians, the average number of corrections per needle will be close to zero. However, observation of medical residents clearly indicates that one to three redirections per needle are common for those with little hands-on experience. For large prostates an implant can contain up to 30 needles and a total number of punctures (initial insertion + redirections) of two to four per needle leads to 60–120 full or partial needle paths. Because of its explicit knowledge of the relevant coordinate systems, a stereotactic robot like the one used for these experiments can execute an implant using only one needle insertion per needle. This would reduce the volume of tissue cut by the needles and therefore has the potential to significantly reduce trauma and puncture-induced edema.

In addition to trauma another factor of standard brachytherapy that can benefit from improved delivery techniques is seed placement uncertainty. This uncertainty can lead to inadequate dose coverage of the target organ or overdosage of the healthy structures. One method to account for uncertainty that is already starting to be implemented in the clinic (7,42), but would benefit from a stereotactic robotic device is *adaptive planning*, in which the plan is modified as more information is gathered during the course of the implant procedure. Foster et al. demonstrated a PPI procedure which allows for updating the dose planning software with the actual position of the placed needle tip immediately after its insertion and prior to dropping the seeds. It is done in this way since the needle is clearly visible on the ultrasound image. The repositioning of the needle tip slightly effects the coordinates of the seeds to be deposited in that pre-loaded needle. This information is automatically registered by the TPS. Westendorp et al. showed that intraoperative adaptive

brachytherapy procedures can have an impact on the dosimetry of the final implant. Both of these procedures allow for more accurate post-implant dosimetry and can allow a physician to determine whether there are parts of the prostate which do not receive a sufficient dose. If so, additional seeds can be placed to fill in the gaps in the coverage. These works suggest a clear impact on toxicity. It has recently been shown that a robotic device can be used in an MR environment to implant individual radioactive seeds in the prostate of live canines (43). In that study, images were acquired and inert seeds locations were determined one-by-one by eye. This study, in contrast, demonstrates that the robot can access the entirety of the generally larger human prostates and used computer-based planning to generate seed positions.

IGRIP brachytherapy requires the integration of a robotic device into the clinical workflow and it is necessary to be able to seamlessly transfer coordinate system information between all the elements in the process. These experiments addressed each element of the workflow depicted in Figure 1:

- Validated the communication of reference systems between imaging, planning, and robotic delivery;
- demonstrated the ability to operate the robot in a clinical CBCT & MR environments;
- demonstrated the ability to use MR Spectroscopy to guide the robot to a target location;
- demonstrated the ability to use the MR-guided robot to deliver a seed to a desired location in non-homogeneous soft tissue (bovine muscle);
- demonstrated the ability to use quasi-real-time image guidance to validate the location of the brachytherapy needle at the delivery site prior to depositing the seed;
- implemented a full brachytherapy treatment procedure in a prostate phantom, including imaging, robot registration to the image coordinate system, generating a dose plan using IPSA, transferring the planned seed coordinates to the robot, delivering the seeds with the robot, and imaging to verify seed placement locations.

Incorporating robots, image guidance, and inverse planning can mitigate the disparity between more-practiced and less-experienced clinicians. Some of the most promising advancements that can immediately be addressed in the current brachytherapy paradigm are reducing needle-puncture-induced edema and improving the conformality of the delivered dose to the diseased tissues through improved seed placement accuracy. However, stereotactic robotics devices will also be able to push brachytherapy into a new paradigm by enabling access to body sites previously unavailable for brachytherapy treatment. The current permanent seed brachytherapy paradigm relies on real-time image guidance and often a pre-fabricated regular-grid template of possible needle positions for placement of the radioactive seeds. Because of this, brachytherapy is mostly limited to areas of the body that have predictable disease topology (prostate cancer), and/or easily accommodate naked-eye or ultrasound imaging: Prostate and gynecological cancers (transrectal ultrasound), eye and skin lesions (naked-eye). However, a stereotactic device – because of its explicit link to the reference frame of the patient – can both do away with the template guide to allow for vastly more degrees of freedom in needle positioning and not require real-time imaging for implantation. This could allow access to a broad range of anatomical sites like the liver, pelvic side wall, or the densely packed structures of the head and neck.

Through the course of the work with this particular robotic device, elements of the robotic design that can still be optimized for use in the clinic were identified. To obtain the best possible access to the prostate target while avoiding sensitive structures, the conical needle pattern was employed, which, along with other robot-deliverable non-standard catheter patterns, has been shown to provide treatment benefits (40). The range of needle angles achievable was limited slightly by the range of motion of the robot in the anteroposterior direction (translation). In addition the range of angles in the anteroposterior direction is adequate for an average human prostate (as exemplified by the CIRS phantom – 30 cc), provided a precise mounting of the robot on the treatment couch is employed. A larger range of motion would allow for less stringent setup positioning. This can be remedied by extending the range of the actuator motors and/or moving the motors closer to each other and will be implemented in the next design of MRBot.

The seed magazine is located on the control device, which can lead to difficulties associated with sterilization and radiation protection. Although the robot is designed such that the same needle is used for the insertion of all seeds and therefore the needle needs only be exchanged at the end of the implant procedure, it may be needed on occasion to exchange the needle. This process requires approximately 15 minutes with the current design: A costly period during an operating room procedure. Finally, the needle insertion mechanism operates on the principle that a fast insertion utilizes the rest inertia of the organs to minimize tissue movement and deformation. However in some circumstances, it would be clinically beneficial to be able to have control of the needle insertion speed. The next version of the robot will be designed to address these issues.

Conclusions

In order to bring a stereotactic robot into the clinic, it must be incorporated into a clinical workflow. This was achieved by demonstrating these proofs of concept:

- The ability to link multiple coordinate systems,
- the ability to guide a needle-placement robot using MR spectroscopy,
- the ability to implement an image guided workflow, and
- the ability to perform image-guided inverse-planned robotic delivery in both CBCT and MRI environments.

An adaptive, image-guided delivery workflow was demonstrated in both MR or CBCT imaging environments. This process allows for needle adjustment (retraction and reinsertion) in the case that the needle is in the wrong position. Also demonstrated was the ability to robotically deliver seeds to locations determined by an anatomy-based seed-location planning system, and the ability of the system to incorporate novel (non-rectangular-template-based) seed/needle patterns that can avoid penetrating sensitive organs (e.g. penile bulb, rectum, urethra) and circumvent the pubic arch.

The MRI-stealth robotic system, MRBot, was used for the first time in a clinical CBCT environment. It was successfully shown that the reference systems of both imaging devices, the brachytherapy planning system, and the robot control can be registered to guide the delivery of a seed to within 2 mm of a target. Various types of targets were used including ceramic dummy brachytherapy seeds, MR-spectroscopy-sensitive metabolite, and a physical model of the anatomy of the prostate region.

Specific limitations of the MRBot when used in an adaptive planning brachytherapy environment were identified – these will be addressed in future designs. On the research side the MRI robot is currently updated for clinical trials of MRI-guided prostate biopsy. For

MRI-guided brachytherapy steps are currently being taken for the development of a commercial system that combines the MRI robot technology with brachytherapy algorithms as presented in this paper.

Acknowledgments

This work was supported in part by the UCSF Department of Radiation Oncology and in part by Nucletron.

References

1. Blasko JC, Mate T, Sylvester JE, Grimm PD, Cavanagh W. Brachytherapy for carcinoma of the prostate: Techniques, patient selection, and clinical outcomes. Seminars in Radiation Oncology. 2002; 12:81–94. [PubMed: 11813153]
2. Potters L, Morgenstern C, Calugaru E, Fearn P, Jassal A, Presser J, et al. 12-year outcomes following permanent prostate brachytherapy in patients with clinically localized prostate cancer. Journal of Urology. 2005; 173:1562–6. [PubMed: 15821486]
3. Thompson I, Thrasher JB, Aus G, Burnett AL, Canby-Hagino ED, Cookson MS, et al. Prostate Cancer Clinical Guideline Update Panel. Guideline for the Management of Clinically Localized Prostate Cancer: 2007 Update. Journal of Urology. 2007; 177:2106–31. [PubMed: 17509297]
4. Zelefsky MJ, Yamada Y, Cohen GN, Shippy A, Chan H, Fridman D, et al. Five-year outcome of Intraoperative Conformal Permanent I-125 Interstitial Implantation for Patients with Clinically Localized Prostate Cancer. Int J Radiat Oncol, Biol Phys. 2007; 67:65–70. [PubMed: 17189063]
5. Pasteau O, Degrais P. The radium treatment of cancer of the prostate. Journal of Urology. 1913; 4:341–66.
6. Holm HH, Pedersen JF, Hansen H, Stroyer I. Transperienal 125I iodine seed implantation in prostatic cancer guided by transrectal ultrasonagraphy. Journal of Urology. 1983; 130:283–6. [PubMed: 6876274]
7. Foster W, Beaulieu L, Harel F, Vigneault AGME. The impact of 3d image guided prostate brachytherapy on therapeutic ratio: the quebec university hospital experience. Cancer/Radiothérapie. 2007; 11:452–60.
8. Lee WR, Hanks GE, Hanlon A. Increasing prostate-specific antigen profile following definitive radiation therapy for localized prostate cancer: clinical observations. Journal of Clinical Oncology. 1997; 15:230–8. [PubMed: 8996147]
9. Chen AB, D'Amico AV, Neville BA, Steyerberg EW, Earle CC. Provider Case Volume and Outcomes Following Prostate Brachytherapy. Journal of Urology. 2009; 181:113–8. [PubMed: 19012905]
10. Stone NN, Stock RG. Complications Following Permanent Prostate Brachytherapy. European Urology. 2002; 41:427–33. [PubMed: 12074815]
11. Stone NN, Potters L, Davis BJ, Ciezki JP, Zelefsky MJ, Roach M, et al. Customized Dose Prescription for Permanent Prostate Brachytherapy: Insights From a Multicenter Analysis of Dosimetry Outcomes. Int J Radiat Oncol, Biol Phys. 2007; 69:1472–7. [PubMed: 17689026]
12. Huang K, Sneed PK, Kunwar S, Kragten A, Larson DA, Berger MS, et al. Surgical resection and permanent Iodine-125 brachytherapy for brain metastases. Journal of Neuro-Oncology. 2009; 91:83–93. [PubMed: 18719856]
13. Cleary K, Watson V, Lindisch D, Taylor RH, Fichtinger G, White CS, et al. Precision placement of instruments for minimally invasive procedures using a "needle driver" robot. The International Journal of Medical Robotics and Computer Assisted Surgery. 2005; 1:40–7.
14. Intuitive Surgical. http://www.intuitivesurgical.com
15. Taylor RH, Stoianovici D. Medical Robotics in Computer-Integrated Surgery. IEEE Transactions on Robotics and Automation. 2003; 19:765–78.
16. Cleary K, Melzer A, Watson V, Kronreif G, Stoianovici D. Interventional robotic systems: applications and technology state-of-the-art. Min Invas Ther & Allied Technol. 2006; 15:101–13.

17. Chinzei, K.; Hata, N.; Jolesz, FA.; Kikinis, R. MR compatible surgical assist robot: System integration and preliminary feasibility study. Medical Image Computing and Computer Assisted Intervention (MICCAI); October 2000; p. 921-30.
18. DiMaio, SP.; Pieper, S.; Chinzei, K.; Hata, N.; Balogh, E.; Fichtinger, G., et al. Robot-assisted needle placement in open-MRI: System architecture, integration and validation. In: Westwood, JD., et al., editors. Medicine Meets Virtual Reality. Vol. 14. Washington, DC: IOS Press; January. 2006 p. 126-131.
19. Stoianovici D, Song D, Petrisor D, Ursu D, Mazilu D, Mutener M, et al. “MRI Stealth” robot for prostate interventions. Min Invas Ther & Allied Technol. 2007; 16:241–8.
20. Fischer, GS.; Iordachita, I.; DiMaio, SP.; Fichtinger, G. Design of a Robot for Transperineal Prostate Needle Placement in MRI Scanner. 2006 IEEE International Conference on Mechatronics; 2006.
21. Lagerburg V, Moerland MA, van Vulpen M, Lagendijk JJW. A new robotic needle insertion method to minimise attendant prostate motion. Radiotherapy and Oncology. 2006; 80:73–7. [PubMed: 16870290]
22. Melzer A, Gutmann B, Remmele T, Wolf R, Lukoscheck A, Bock M. Innomotion for percutaneous image-guided interventions. IEEE Engineering in Medicine and Biology Magazine. 2008:66–73. [PubMed: 18519184]
23. Moerland MA, Van den Bosch MR, Lagerburg V, Battermann JJ, Van Vulpen M, Lagendijk JJW. An MRI scanner compatible implant robot for prostate brachytherapy. Brachytherapy. 2008; 7:100.
24. Goldenberg AA, Trachtenberg J, Yi Y, Weersink R, Sussman MS, Haider M, et al. Robot-assisted MRI-guided prostatic interventions. Robotica. 2010; 28:215–24.
25. Stoianovici D, Patriciu A, Petrisor D, Mazilu D, Kavoussi L. A new type of motor: Pneumatic step motor. IEEE/ASME Trans Mechatronics. 2007; 12:98–106.
26. Kurhanewicz J, Swanson MG, Nelson SJ, Vigneron DB. Combined magnetic resonance imaging and spectroscopic imaging approach to molecular imaging of prostate cancer. Journal of Magnetic Resonance Imaging. 2002; 16:451–63. [PubMed: 12353259]
27. Kurhanewicz J, Vigneron DB, Hricak H, Narayan P, Carroll P, Nelson SJ. Three-dimensional H-1 MR Spectroscopic Imaging of the in Situ Human Prostate with High (0.24–0.7 cm3) Spatial Resolution. Radiology. 1996; 198:795–805. [PubMed: 8628874]
28. Lessard E, Pouliot J. Inverse planning anatomy-based dose optimzation for HDR-brachytherapy of the prostate using fast simulated annealing algorithm and dedicated objective function. Medical Physics. 2001; 28:773–9. [PubMed: 11393472]
29. Lessard E, Hsu IC, Pouliot J. Inverse planning for interstitial gynecologic template brachytherapy: truly anatomy-based planning. Int J Radiat Oncol, Biol Phys. 2002; 54:1243–51. [PubMed: 12419454]
30. Pouliot, J.; Lessard, E.; Hsu, IC. AAPM, Medical Physics Monograph. 2. Seattle, WA: 2005. Advanced 3D Planning in Brachytherapy, chapter 21: Brachytherapy Physics.
31. Lessard E, Kwa SLS, Pickett B, Roach M III, Pouliot J. Class solution for inversely planned permanent prostate implants to mimic an experienced dosimetrist. Medical Physics. 2006; 33:2773–82. [PubMed: 16964853]
32. Patriciu A, Petrisor D, Muntener M, Mazilu D, Schar M, Stoianovici D. Automatic brachytherapy seed placement under MRI guidance. IEEE Trans Biomedical Engineering. 2007; 54:1499–1506.
33. CIRS Tissue Simulation & Phantom Technology. http://cirsinc.com/
34. Lagerburg V, Moerland MA, Lagendijk JJW, Battermann JJ. Measurement of prostate rotation during insertion of needles for brachytherapy. Radiotherapy and Oncology. 2005; 77:318–23. [PubMed: 16289399]
35. Chentanez, N.; Alterovitz, R.; Ritchie, R.; Cho, L.; Hauser, KK.; Goldberg, K., et al. Interactive Simulation of Surgical Needle Insertion and Steering. Computer Graphics Proceedings, Annual Conference Series; 2009.
36. van Gellekom MPR, Moerland MA, Battermann JJ, Lagendijk JJW. MRI-guided prostate brachytherapy with single needle method—a planning study. Radiotherapy and Oncology. 2004; 71:327–32. [PubMed: 15172149]

37. Fu L, Ng WS, Liu H, O'Dell W, Rubens D, Strang J, et al. Bouquet brachytherapy: Feasibility and optimization of conically spaced implants. Brachytherapy. 2005; 4:59–63. [PubMed: 15737908]

38. Fu L, Liu H, Ng WS, Rubens D, Strang J, Messing E, et al. Hybrid dosimetry: Feasibility of mixing angulated and parallel needles in planning prostate brachytherapy. Medical Physics. 2006; 33:1192–8. [PubMed: 16752554]

39. van den Bosch MR, Lips IM, Lagerburg V, van Vulpen M, Lagendijk JJW, Moerland MA. Feasibility of adequate dose coverage in permanent prostate brachytherapy using divergent needle insertion methods. Radiotherapy and Oncology. 2008; 86:120–5. [PubMed: 18037520]

40. Cunha JAM, Hsu IC, Pouliot J. Dosimetric equivalence of nonstandard HDR brachytherapy catheter patterns. Medical Physics. 2009; 36:233–9. [PubMed: 19235391]

41. Munarriz RM, Yan QR, Nehra A, Udelson D, Goldstein I. Blunt trauma: The pathophysiology of hemodynamic injury leading to erectile dysfunction. Journal of Urology. 1995; 153:1831–40. [PubMed: 7752329]

42. Westendorp H, Hoekstra CJ, van't Riet A, Minken AW, Immerzeel JJ. Intraoperative adaptive brachytherapy of iodine-125 prostate implants guided by c-arm cone-beam computed tomography-based dosimetry. Brachytherapy. 2007; 6:231–7. [PubMed: 17991620]

43. Muntener M, Patriciu A, Petrisor D, Schaar M, Ursu D, Song DY, et al. Transperineal Prostate Intervention: Robot for Fully Automated MR Imaging—System Description and Proof of Principle in a Canine Model. Radiology. 2008; 247:543–9. [PubMed: 18430882]

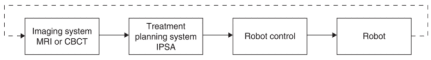

Figure 1.

An adaptive robotic brachytherapy image/plan/begin-delivery/image/plan/finish-delivery information workflow. This workflow begins with the acquisition of an MR or CT set of images of the patient. These images are then transferred via DICOM format to a treatment planning system where the anatomy is contoured and the needle and seed locations (i.e. a *dose plan*) are determined. The dose plan is transferred to the robot control unit which executes the instructions necessary to position the robot to insert the needles and deliver the seeds. Prior to placing all the seeds, an *adaptive planning* would entail returning to the beginning of the workflow to re-image the patient, determine the actual position of the already-placed seeds, and re-plan the remaining seeds if necessary to fine tune the dose distribution. Note, ultrasound is not included in the figure because adaptive brachytherapy requires the visualization of already-placed seeds. Identifying and locating seeds using ultrasound images is extremely difficult: Post-implant dosimetry is routinely done using CT imaging.

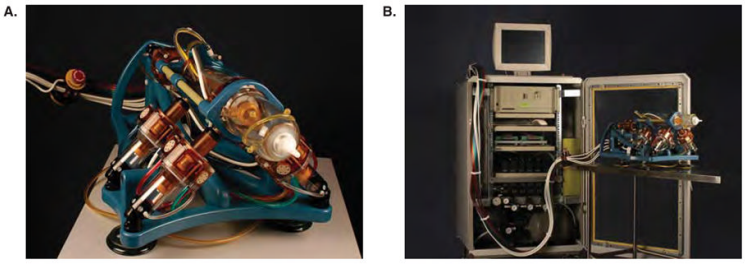

Figure 2.
The MRBot robotic brachytherapy seed delivery system: (a) The robot is designed to fit inside a closed-bore MR system and is fully MR compatible, (b) the robot is attached to the control unit via air tubes and fiber optic cables.

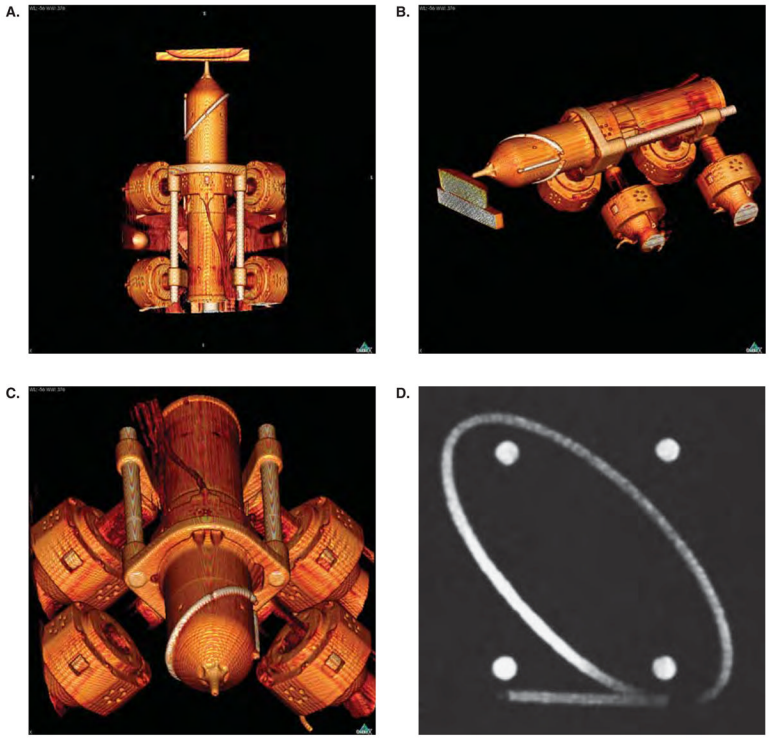

Figure 3.
CT scan of the robot. Note the lack of artifacts that would be induced by materials with a high atomic number and which would show up as dense white streaks on the images. The end effector is positioned at the surface of a gel phantom (a,b). An ellipse, a line, and four balls are embedded on the end effector of the robot as registration markers. They can be seen clearly on the CBCT images (a,b,c); they are also visible under MR (d).

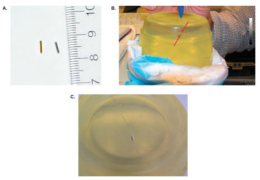

Figure 4.
Robot registration in the MR environment using a gel phantom; (a) the gold marker seed (left) to be implanted in the test media is 4 mm in length. It will show a stronger signal on the CBCT than the steel dummy seed (right); (b) the target and robot-placed seeds are indicated by the arrows in the center of the gel. The needle track is visible: the target track enters from the left and the dummy seed from the right; (c) gel phantom with ceramic target seed (on right, white) and robot-placed steel seed (left).

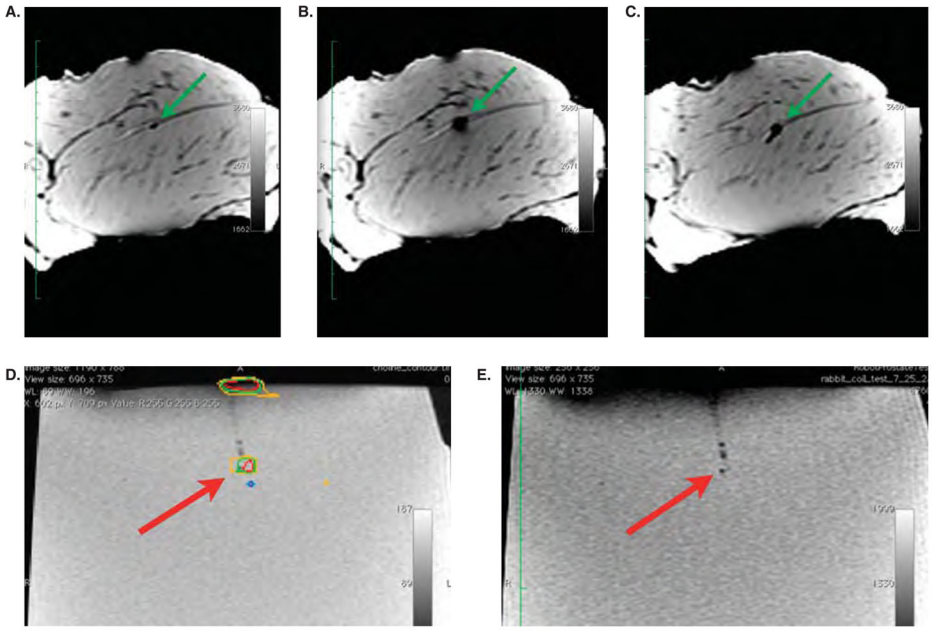

Figure 5.
Test of robot registration in a non-homogeneous (bovine muscle) environment and test of robot registration using MRS imaging to define the target in a gel phantom with MRS-imageable metabolite: (a) The target location is indicated by the arrow. (b) The robot's needle has been inserted (orientated into the plane of the page) to the target location. (c) The seed has been dropped and the needle retracted. (d) The target as defined by the MRS analysis. (e) Robot needle is inserted to the location defined by the choline. The seed is laterally located 2 mm from the target location. The center of the seed is one slice in front of the slice shown. With a slice thickness of 2 mm, the seed was placed within 3 mm of the target.

Figure 6.
(a) The robot on the CBCT couch. Note the open architecture of the CBCT imaging device. This allowed for easy mechanical access and visual inspection at every step of the procedure. (b) The robot on the couch of the conebeam CT system with the needle inserted in the phantom.

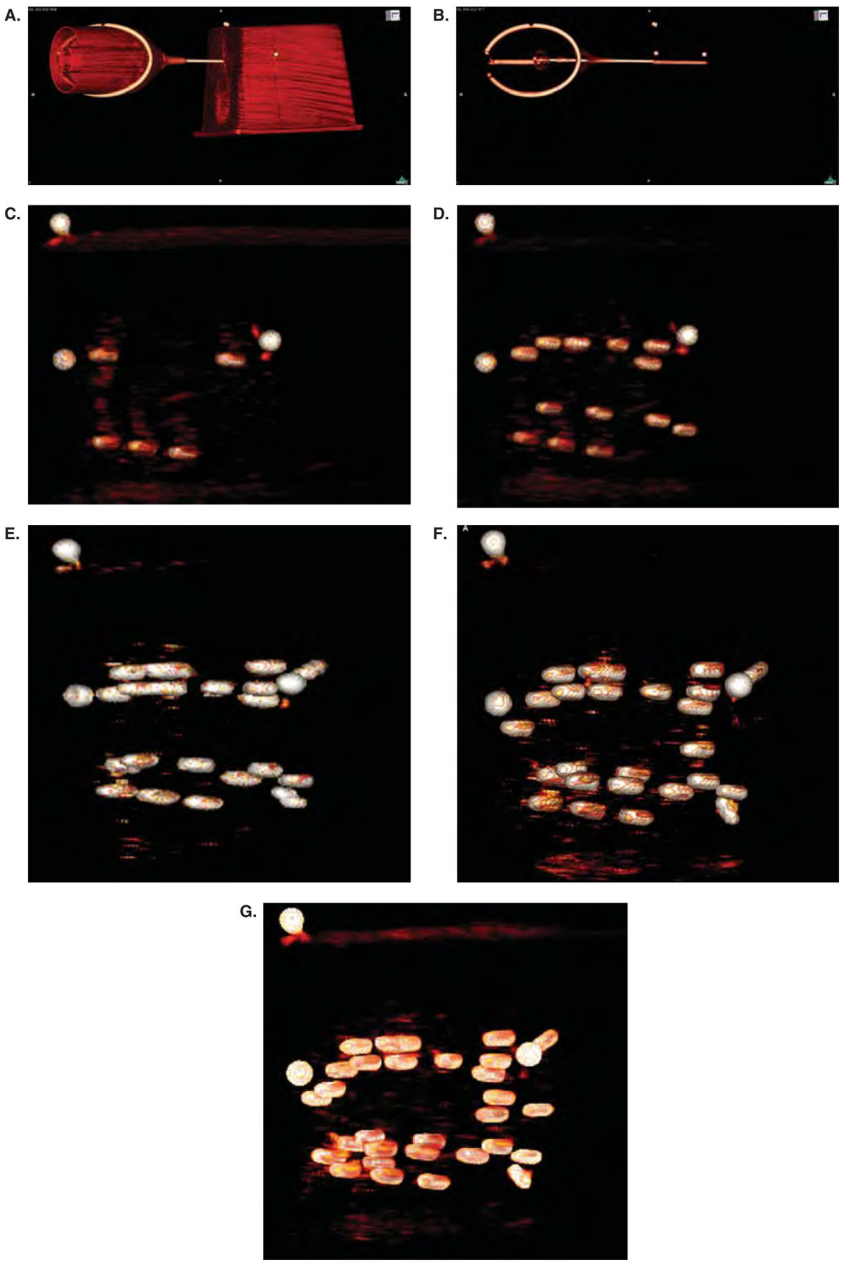

Figure 7.

Intra-operative verification of the placement of PPI seeds. Panels a and b show the robot head with the needle extended along with the phantom. The contrast window level has been modified in panel b compared to panel a to show the internal structure of the phantom. The three round white dots above the needle (easily seen in panel b) were glued to the outside surface of the phantom – they can be seen in each figure and serve as a reference point. Panel c, d, e, f, and g were taken after two, four, six, eight, and all ten needles, respectively, were placed. These figures show the ease of which the seeds can be identified in the CT environment. In contrast, reliable seed identification is nearly impossible using ultrasound imaging techniques.